Autoimmunity-associated protein tyrosine phosphatase PEP negatively regulates IFN-α receptor signaling

Derek A. Holmes,[1] Eric Suto,[2] Wyne P. Lee,[2] Qinglin Ou,[1] Qian Gong,[1] Hamish R.C. Smith,[1] Patrick Caplazi,[3] and Andrew C. Chan[1]

[1]Department of Immunology, [2]Department of Translational Immunology, and [3]Department of Pathology, Genentech, Inc., South San Francisco, CA 94080

The protein tyrosine phosphatase *PTPN22(C1858T)* allelic polymorphism is associated with increased susceptibility for development of systemic lupus erythematosus (SLE) and other autoimmune diseases. *PTPN22* (also known as LYP) and its mouse orthologue PEP play important roles in antigen and Toll-like receptor signaling in immune cell functions. We demonstrate here that PEP also plays an important inhibitory role in interferon-α receptor (IFNAR) signaling in mice. PEP co-immunoprecipitates with components of the IFNAR signaling complex. *Pep*$^{-/-}$ hematopoietic progenitors demonstrate increased IFNAR signaling, increased IFN-inducible gene expression, and enhanced proliferation and activation compared to *Pep*$^{+/+}$ progenitors in response to IFN-α. In addition, *Pep*$^{-/-}$ mice treated with IFN-α display a profound defect in hematopoiesis, resulting in anemia, thrombocytopenia, and neutropenia when compared to IFN-α–treated *Pep*$^{+/+}$ mice. As SLE patients carrying the *PTPN22(C1858T)* risk variant have higher serum IFN-α activity, these data provide a molecular basis for how type I IFNs and PTPN22 may cooperate to contribute to lupus-associated cytopenias.

CORRESPONDENCE
Andrew C. Chan:
acc@gene.com

Abbreviations used: 5-FU, 5-fluorouracil; BAFF, B cell activating factor; BLys, B lymphocyte stimulator; BMDM, BM-derived macrophage; CMP common myeloid progenitor; GMP, granulocyte myeloid progenitor; HCV, hepatitis C virus; HSC, hematopoietic stem cell; IFNAR, IFN-α receptor; JAK, Janus kinase; MEP, megakaryocyte/erythrocyte progenitor; MPP, multipotent progenitor; PLT, platelet; PTK, protein tyrosine kinase; SLE, systemic lupus erythematosus; SNP, single nucleotide polymorphism; STAT, signal transducer and activator of transcription; TLR, toll-like receptor.

Systemic lupus erythematosus (SLE) is a prototype systemic autoimmune inflammatory disorder characterized by the production of autoantibodies, immune complex formation, and immune complex deposition in end-organs that contribute to skin rash, nephritis, arthritis, cerebritis, and vasculitis. Hematologic abnormalities are also amongst the most common manifestation in SLE and include anemia, thrombocytopenia, neutropenia, and lymphopenia (Bashal, 2013). Autoantibodies against RBCs, platelets (PLTs), lymphocytes, and neutrophils, as well as reduced expression of complement regulatory proteins CD55 and CD59 making cells more susceptible to complement-mediated lysis, account for some cytopenias, but the etiology of many remain unknown (Mittal et al., 1970; Butler et al., 1972; García-Valladares et al., 2006). BM abnormalities, including dyserythropoiesis, hypocellularity, and myelofibrosis, are commonly found and lend support for the contribution of chronic immune activation to BM dysfunction (Voulgarelis et al., 2006).

Genome-wide association studies have identified >40 confirmed genetic loci associated with the development of SLE (Cui et al., 2013). The *PTPN22(C1858T)* polymorphism, resulting in a missense mutation R620W, is associated with increased risk of developing type I diabetes (Bottini et al., 2004), SLE (Kyogoku et al., 2004), rheumatoid arthritis (Begovich et al., 2004), Graves' disease (Velaga et al., 2004), and other autoimmune disorders (Stanford and Bottini, 2014; Rawlings et al., 2015). PTPN22/LYP and its mouse orthologue PEP are members of the PEST-domain containing nonreceptor protein tyrosine phosphatase family and play important roles in TCR, BCR, IFN-γ receptor, and Toll-like receptor (TLR) functions (Rhee and Veillette, 2012; Spalinger et al., 2013; Wang et al., 2013; Bottini and Peterson, 2014). Whereas the human *PTPN22(C1858T)* at-risk SNP has been proposed to have both activating and inhibitory functions, recent studies of knock-in mice expressing the mouse PEP(R619W) orthologue support a loss-of-function phenotype and mimic

The Rockefeller University Press $30.00
J. Exp. Med. 2015 Vol. 212 No. 7 1081–1093
www.jem.org/cgi/doi/10.1084/jem.20142130

The Journal of Experimental Medicine

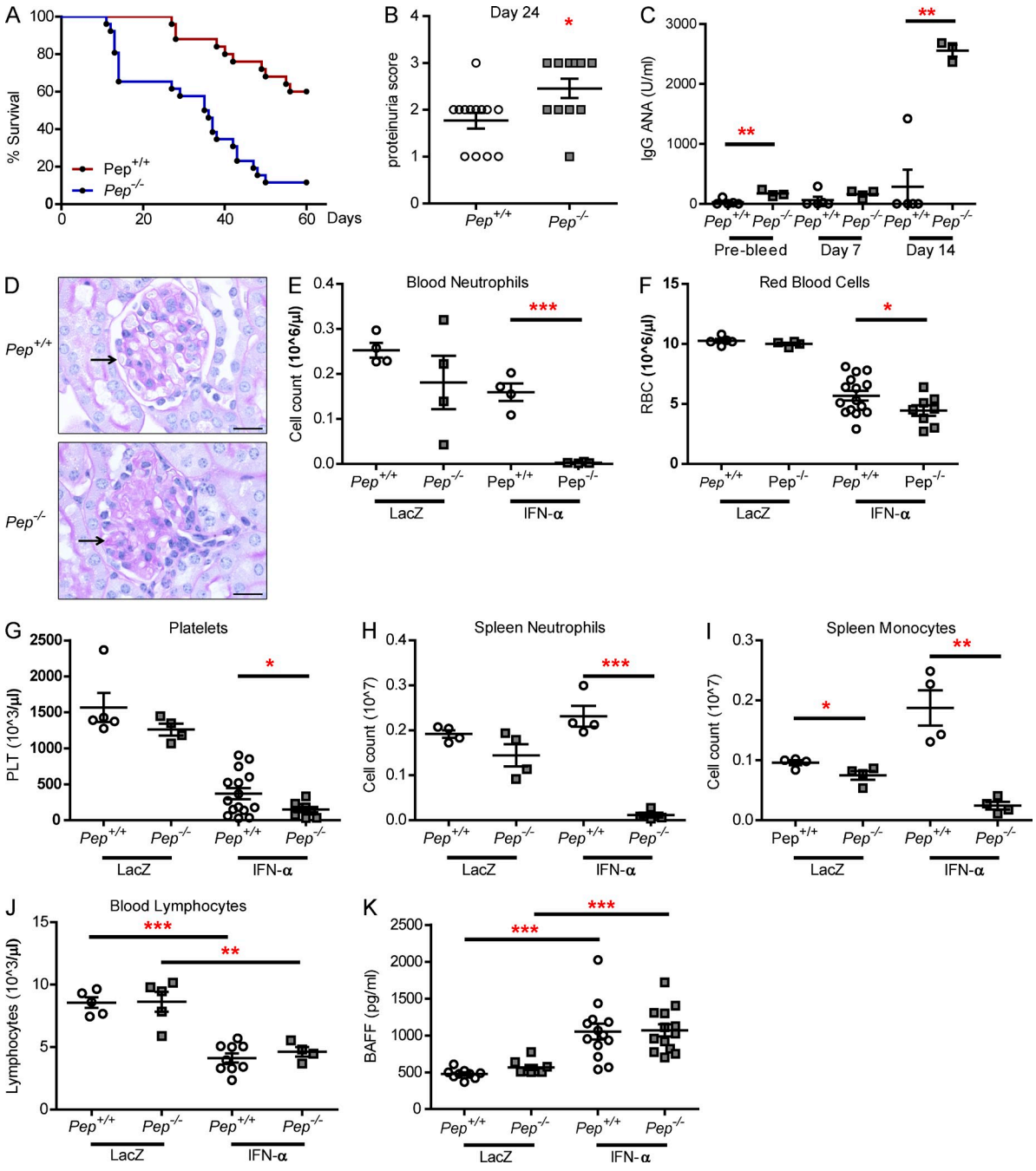

Figure 1. ***Pep*$^{-/-}$ mice are susceptible to an IFN-α–mediated lupus-like disease.** (A) *Pep*$^{+/+}$ (red) and *Pep*$^{-/-}$ (blue) mice were injected i.v. with adenovirus expressing IFN-α5 (Ad5-IFN-α5, 10^9 PFU/mouse). Mortality was observed for 60 d after infection. Survival curves represent a total of 25 mice per genotype from 3 independent experiments. (B) Protein levels in the urine were measured in Ad5-IFN-α5 (10^9 PFU/mouse)–infected *Pep*$^{+/+}$ (open circles) and *Pep*$^{-/-}$ (grey squares) mice 24 d after infection. Data are cumulative of 3 independent experiments representing a total of 11 *Pep*$^{+/+}$ or 13 *Pep*$^{-/-}$ mice. (C) Serum from Ad5-IFN-α5 (10^9 PFU/mouse)–infected *Pep*$^{+/+}$ (open circles) and *Pep*$^{-/-}$ (grey squares) mice was analyzed at the indicated times for antinuclear IgG antibodies by ELISA. n = 3–5 mice/group and data shown are representative of 3 independent experiment. (D) Kidney sections from *Pep*$^{+/+}$ (top) and *Pep*$^{-/-}$(bottom) mice infected with Ad5-IFN-α5 (10^9 PFU/mouse) 24 d after infection were stained with PAS. Arrows indicate capillary basement membranes and mesangial matrix. Bar, 20 µm. Images are representative of 12–20 sections per genotype from 2 independent experiments. (E–G) Blood neutrophil (E), RBC (F), and PLT (G) numbers from *Pep*$^{+/+}$ (open circles) and *Pep*$^{-/-}$ (grey squares) were analyzed in Ad5-LacZ (10^9 PFU/mouse) or Ad5-IFN-α5 (10^9 PFU/mouse) at 14 (E) or 28 d (F–G) after infection. (E) n = 4 mice/group and data shown are representative of 3 independent experiments; (F–G) n = 5 mice/group in LacZ-treated cohort and data shown are representative of 3 independent experiments. n = 25 *Pep*$^{+/+}$ and 8 *Pep*$^{-/-}$ mice in the IFN-α5 cohorts. Data shown are cumulative of three independent experiments. (H and I) Splenic neutrophil (H) and monocyte (I) numbers in *Pep*$^{+/+}$ (open circles) and *Pep*$^{-/-}$ (grey squares) mice were analyzed in control Ad5-LacZ (10^9 PFU/mouse) or Ad5-IFN-α5 (10^9 PFU/mouse) 14 d after infection.

Pep$^{-/-}$ mice (Vang et al., 2005; Rieck et al., 2007; Zikherman et al., 2009; Zhang et al., 2011; Dai et al., 2013; Rawlings et al., 2015). *Pep*$^{-/-}$ mice develop splenomegaly and spontaneous germinal center formation as they age and are prone to, but do not develop, systemic autoimmunity (Hasegawa et al., 2004). Consistent with the multifactorial nature of human SLE, development of autoimmunity and clinical disease requires additional genetic and exogenous factors. Whereas *Pep*$^{-/-}$ mice on a C57BL/6 background do not develop systemic autoimmunity (Hasegawa et al., 2004), *Pep*$^{-/-}$ mice expressing a CD45(E613R) mutation develop autoantibodies, glomerulonephritis, and increased mortality despite being on a nonautoimmune-prone background (Zikherman et al., 2009).

Type I IFNs have long been implicated in human SLE pathogenesis as a subset of patients treated with IFN-α for chronic HCV or cancers develop drug-induced lupus (Ho et al., 2008). As with PTPN22, polymorphisms in transcription factors that regulate type 1 IFN—*IRF5* (OR = 1.3–1.8), *IRF7* (OR = 1.3), *IRF8* (OR = 1.17–1.28; Harley et al., 2008; Hom et al., 2008; Gateva et al., 2009; Han et al., 2009; Chung et al., 2011; Cunninghame Graham et al., 2011; Lessard et al., 2012), and *TYK2* (OR = 1.29), a protein tyrosine kinase (PTK) requisite for IFNAR function (Cunninghame Graham et al., 2011)—are associated with increased SLE susceptibility. A type 1 IFN-inducible gene signature has been reported in SLE and a higher magnitude of the IFN-induced gene signature is associated with greater propensity to develop renal, central nervous system, and hematologic manifestations (Baechler et al., 2003). SLE patients carrying the *PTPN22(C1858T)* at-risk polymorphism have higher IFN-α levels and higher IFN-α levels correlate inversely with leukocyte numbers (Bengtsson et al., 2000; Kariuki et al., 2008). Finally, treatment of patients with an anti–IFN-α mAb (rontalizumab) results in improvement in the Systemic Lupus Responder Index and enables more patients to reduce their concomitant corticosteroid use (Kalunian et al., 2015).

Mouse models of SLE also support a pathogenic role for type I IFNs. Administration of IFN-α recombinant protein (Heremans et al., 1978; Adam et al., 1980), infection with viral-mediated IFN-α expression (Mathian et al., 2005) or administration of poly(I:C) (Carpenter et al, 1970) accelerate autoimmunity in NZB/W F1 mice. NZB mice lacking IFNAR do not develop anti-RBC autoantibodies and are protected from the development of autoimmune hemolytic anemia (Santiago-Raber et al., 2003). Similarly, lack of IFNAR attenuates lupus manifestations in other models of lupus, including NZM2328 and B6.Nba.2 (Jørgensen et al., 2007; Agrawal et al., 2009). Finally, administration of an anti-IFNAR mAb in BXSB male mice improves serologic, cellular, and histologic parameters of lupus, and also extends survival (Baccala et al., 2012).

Type I IFNs are rapidly up-regulated after infection and serve as a first line of innate immune defense. Type I IFNs have pleiotropic effects on hematopoietic and nonhematopoietic cells to control immunity, induce viral inhibitory activities and regulate hematopoiesis. In immune cells, type 1 IFNs induce monocyte differentiation, augment antigen presentation by dendritic cells, promote T cell survival, increase T cell cytolysis, and enhance B cell differentiation and antibody production (Hall and Rosen, 2010). IFN-α has also recently emerged as an important regulator of hematopoiesis. In addition to immunomodulatory effects, IFN-α mobilizes hematopoietic stem cells (HSCs) to proliferate from a quiescent state to a renewal state. However, chronic activation of the IFN-α pathway results in HSC exhaustion and impairs HSC functions (Essers et al., 2009).

Given the association of PTPN22 and IFN-α in SLE (Kariuki et al., 2008), we investigated the effects of IFN-α in *Pep*$^{-/-}$ mice. These studies reveal a previously unrecognized role for PEP as a negative regulator of IFNAR-mediated activation in hematopoietic progenitors and provides a mechanistic basis by which PEP and IFN-α may contribute to hematopoietic dysfunction in SLE.

RESULTS

PEP deficiency accelerates IFN-α–induced lupus-like disease

Given the genetic links implicating both IFN-α and PTPN22 in human SLE, we tested whether PEP deficiency may affect the ability of IFN-α to induce SLE. Systemic administration of IFN-α5 (10^9 PFU/mouse) by adenoviral delivery resulted in 40% mortality in *Pep*$^{+/+}$ mice (C57BL/6 background) 2 mo after IFN-α administration (Fig. 1 A). In contrast, IFN-α (10^9 PFU/mouse) treated *Pep*$^{-/-}$ mice (C57BL/6) demonstrated 40% mortality by 2 wk and ~90% mortality by 2 mo. Corresponding with increased mortality, IFN-α5–treated *Pep*$^{-/-}$ mice developed increased proteinuria, a mild glomerulopathy, antinuclear autoantibodies. and cytopenias when compared to IFN-α5–treated *Pep*$^{+/+}$ mice (Fig. 1, B–G). Affected glomeruli of IFN-α5–treated *Pep*$^{-/-}$ mice have segmental or global thickening of capillary basement membranes and increased mesangial matrix (Fig. 1 D, arrows), resulting in markedly narrowed capillary profiles. Using an arbitrary scoring system (described in Materials and methods), the pathology score for IFN-α5–treated *Pep*$^{+/+}$ mice was 0.0 ± 0, whereas IFN-α5–treated *Pep*$^{-/-}$ mice was 0.67 ± 0.2 ($P = 0.03$). Cytopenias,

Data are representative of three independent experiments ($n = 4$ mice/group). (J) Blood lymphocyte numbers from *Pep*$^{+/+}$ (open circles) and *Pep*$^{-/-}$ (grey squares) mice were analyzed in Ad5-LacZ (10^9 PFU/mouse) or Ad5-IFN-α5 (10^9 PFU/mouse) 28 d after infection. $n = 4$ mice/group in the LacZ-treated cohort; $n = 9$ *Pep*$^{+/+}$ and 5 *Pep*$^{-/-}$ mice in the IFN-α5–treated cohort. Data shown are representative of three independent experiments. (K) Serum BAFF/BLys levels in *Pep*$^{+/+}$ (open circles) and *Pep*$^{-/-}$ (grey squares) mice were analyzed in control Ad5-LacZ (10^9 PFU/mouse) or Ad5-IFN-α5 (10^9 PFU/mouse) 28 d after infection by ELISA. $n > 13$ mice/group and are cumulative of at least 3 independent experiments. Values in all graphs represent means ± SEM. Statistical analyses were done by two-tailed paired Student's *t* test; *, $P < 0.05$; **, $P < 0.01$; ***, $P < 0.001$.

including peripheral neutropenia, anemia, and thrombocytopenia, as well as reductions in splenic neutrophils and monocytes, were also more severe in IFN-α5–treated $Pep^{-/-}$ mice (Fig. 1, E–I). In contrast, whereas IFN-α5 reduced peripheral lymphocytes, there were no differences between IFN-α5–treated $Pep^{+/+}$ and $Pep^{-/-}$ mice (Fig. 1 J). As IFN-α increased serum BAFF/BLys (Mathian et al., 2005), a key pathogenic factor in SLE, BAFF/BLys levels were elevated in IFN-α5–treated mice compared to LacZ controls, but no differences were observed between IFN-α5–treated $Pep^{+/+}$ and $Pep^{-/-}$ mice (Fig. 1 K). Together, these data suggest that PEP deficiency accelerates IFN-α5–induced lupus-like disease with increased mortality, proteinuria, glomerulopathy, autoantibody production, and cytopenias.

Since a type I IFN gene signature in peripheral blood mononuclear cells is associated with cytopenias in human lupus patients (Baechler et al., 2003), we further dissected the underlying pathogenesis and analyzed the effects of IFN-α on the hematopoietic progenitor compartment. Consistent with the previous description that Sca-1 is an IFN-α–induced activation marker (Essers et al., 2009), we observed increased Sca-1 expression on $Pep^{+/+}$ $cKit^+$ progenitors after IFN-α treatment (unpublished data). Although no differences in HSC and progenitor populations were observed between $Pep^{+/+}$ and $Pep^{-/-}$ mice under homeostatic conditions (unpublished data), a significant reduction in HSC, multipotent progenitor (MPP2 and MPP3), megakaryocyte/erythrocyte progenitor (MEP), and myeloid progenitor (CMP and GMP) populations was observed in IFN-α5–treated $Pep^{-/-}$ mice compared to IFN-α5–treated $Pep^{+/+}$ mice (Fig. 2, A and B). This effect was dose dependent, as administration of 10-fold less (10^8 PFU/mouse) Ad5-IFN-α5 did not affect the HSC population in $Pep^{-/-}$ mice, though the more differentiated multipotent progenitors (MPP2 and MPP3) and myeloid progenitors (CMP/GMP) populations were still reduced in IFN-α5–treated $Pep^{-/-}$ mice (Fig. 2, C and D). There was also a trend in the reduction of LS^-K and MEP cells that did not reach statistical significance. Treatment with Ad5-IFN-α5 (10^8 PFU/mouse) did not result in mortality in either $Pep^{+/+}$ or $Pep^{-/-}$ mice within a 60-d period (unpublished data). Similar effects were observed with administration of poly(I:C) with reduced cellularity in the more differentiated myeloid progenitors (MEP, CMP and GMP) in poly(I:C)-treated $Pep^{-/-}$ mice (Fig. 2, E and F). Consistent with enhanced progenitor activation, we observed increased Sca-1 expression on poly(I:C)-treated $cKit^+$ $Pep^{-/-}$ progenitors compared to $Pep^{+/+}$ progenitors (Fig. 2 G). Together, these observations are consistent with increased activation and potential exhaustion of hematopoietic progenitors in $Pep^{-/-}$ mice after IFN-α treatment.

$Pep^{-/-}$ hematopoietic progenitors demonstrated increased activation and proliferation after IFN-α administration

Previous studies have shown that chronic type I IFN stimulation induces hematopoietic progenitors to proliferate and lose self-renewal capacity, resulting in exhaustion and HSC dysfunction (Essers et al., 2009). To investigate the mechanism leading to decreased numbers of progenitor cells in $Pep^{-/-}$ BM after IFN-α treatment, we assessed BrdU incorporation by progenitor cells as a measure of progenitor proliferation. Consistent with increased activation observed in poly(I:C)-treated mice (Fig. 2 G), $Pep^{-/-}$ myeloid progenitors incorporated BrdU at a higher rate compared to $Pep^{+/+}$ progenitors in poly(I:C)-treated mice (Fig. 3 A). We observed a similar increase in BrdU in $Pep^{-/-}$ compared to $Pep^{+/+}$ myeloid progenitors after low-dose Ad5-IFN-α5 (10^7 PFU/mouse) administration (Fig. 3 B). This increased proliferation in $Pep^{-/-}$ LS^-K, MEP, and CMP/GMP progenitors were associated with increased entry into the cell cycle after poly(I:C) treatment (Fig. 3, D–F). In contrast, no differences in BrdU incorporation or cell cycling were detected between $Pep^{+/+}$ and $Pep^{-/-}$ HSC progenitors (LSK) after poly(I:C) treatment (Fig. 3 C).

To analyze the in vivo consequences of increased proliferative capacity of the $Pep^{-/-}$ hematopoietic progenitors, mice were treated with the chemotherapeutic agent 5-fluorouracil (5-FU) to kill actively proliferating cells. Previous work has demonstrated that repeated poly(I:C) infection to induce chronic systemic IFN-α, followed by 5-FU administration results in BM failure and death due to loss of HSC self-renewal (Essers et al., 2009). $Pep^{-/-}$ mice administered a single dose of poly(I:C), followed by 5-FU, had 33% mortality (Fig. 3 G). In contrast, all $Pep^{+/+}$ mice treated with poly(I:C) were able to compensate and recover after the chemotherapeutic challenge. The greater sensitivity of $Pep^{-/-}$ progenitors to IFN-α was not due to an intrinsic proliferation defect in $Pep^{-/-}$ progenitors, since both $Pep^{+/+}$ and $Pep^{-/-}$ mice, in the absence of poly(I:C), had similar mortality after chronic 5-FU treatment (Fig. 3 H). Thus, our data suggests that PEP regulates the proliferation of hematopoietic progenitors during IFN-α–mediated stress hematopoiesis.

To determine the hematopoietic requirement for PEP in IFN-α–mediated hematopoietic progenitor proliferation, we generated mixed BM chimeras by transferring $Pep^{+/+}$ or $Pep^{-/-}$ donor ($CD45.2^+$) BM competitively with host ($CD45.1^+$) BM at a 1:1 ratio. Reconstituted chimeric mice were treated with poly(I:C) and administered BrdU 24 h later. Donor-derived $CD45.2^+$ $Pep^{-/-}$ myeloid progenitors (LS^-K) incorporated more BrdU compared to donor-derived $CD45.2^+$ $Pep^{+/+}$ myeloid progenitors (Fig. 4 A, left graph). In contrast, host-derived ($CD45.1^+$) myeloid progenitors (LS^-K) incorporated BrdU equivalently (Fig. 4 A, right graph).

To assess the contribution of IFNAR for progenitor activation, we generated competitive BM chimeric mice with donor-derived ($CD45.2^+$) $Pep^{-/-}$ or $Pep^{-/-}IFNAR^{-/-}$ at a 1:1 ratio with host-derived ($CD45.1^+$). Chimeric mice were treated with poly(I:C) for 24 h, and up-regulation of Sca-1 on $cKit^+$ progenitors was analyzed by FACS. Although $Pep^{-/-}$ $cKit^+$ progenitors up-regulated Sca-1 after poly(I:C) treatment (Fig. 4 B, compare left and middle), $Pep^{-/-}IFNAR^{-/-}$ progenitors had reduced Sca-1 up-regulation compared to $Pep^{-/-}$ progenitors in poly(I:C)-treated mice (Fig. 4 B, compare middle and right). In addition, whereas $Pep^{-/-}$ mice

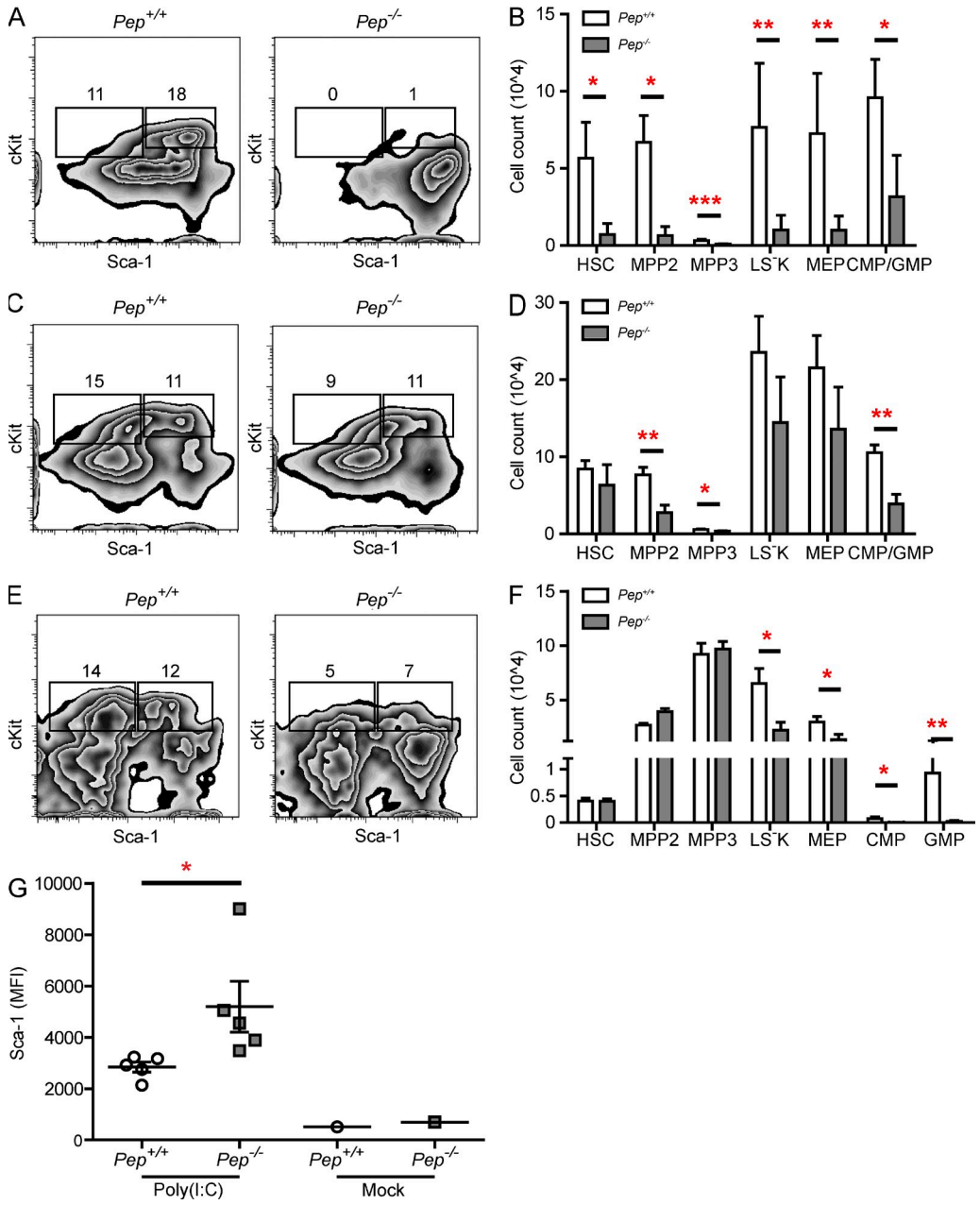

Figure 2. Decreased BM hematopoietic progenitors in *Pep*$^{-/-}$ mice are observed after IFN-α induction. (A–D) *Pep*$^{+/+}$ and *Pep*$^{-/-}$ mice were infected with Ad5-IFN-α5 (10^9 PFU/mouse [A and B] or 10^8 PFU/mouse [C and D]). BM progenitor composition was analyzed 14 d after infection. Lineage$^-$ cells were gated on cKit and Sca-1 to analyze early hematopoietic progenitors (HSC, MPP2, and MPP3) in the Lin$^-$ Sca-1$^+$ cKit$^+$ (LSK) population. Megakaryocyte, erythrocyte progenitors (MEP), and myeloid progenitors (CMP/GMP) were analyzed in the Lin$^-$ Sca-1$^-$ cKit$^+$ (LS$^-$K) populations. BM progenitors from A and C were enumerated from *Pep*$^{+/+}$ (open bar) and *Pep*$^{-/-}$ (grey bar) mice on day 14 after infection with Ad5-IFN-α5 (10^9 PFU/ml [B]; 10^8 PFU/ml [D]). (E and F) Mice were injected i.p. with poly(I:C) (200 µg/mouse) and BM progenitor composition analyzed after 24 h as described in A–D. HSC, LSK CD150$^+$ CD34$^-$CD48$^-$; MPP2, LSK CD150$^+$CD34$^+$CD48$^-$; MPP3, LSK CD150$^+$CD34$^+$CD48$^+$; MEP, LS$^-$K CD16/19$^-$CD34$^-$; CMP, LS$^-$K CD16/CD19^{int}CD34$^+$; GMP, LS$^-$K CD16/19^{hi}CD34$^+$. (G) Sca-1 expression on total cKit$^+$ BM cells was quantitated by fluorescence intensity. *Pep*$^{+/+}$ (open circle) and *Pep*$^{-/-}$ (grey square) mice were treated with poly(I:C) for 24 h and BM progenitors analyzed by FACS. $n = 5$ mice/group in the poly(I:C)-treated cohort. $n = 5$ mice/genotype for all experiments. Data shown are representative of three independent experiments for A and E, and two independent experiments for C. Values in all graphs represent means ± SEM. Statistical analysis was done by two-tailed paired Student's *t* test; *, $P < 0.05$; **, $P < 0.01$; ***, $P < 0.001$.

treated with poly(I:C) had reduced percentage of LS$^-$K progenitors when compared to untreated *Pep*$^{-/-}$ mice, *Pep*$^{-/-}$ *IFNAR*$^{-/-}$ mice treated with poly(I:C) had a similar percentage of LS$^-$K progenitors compared to untreated *Pep*$^{-/-}$ mice (Fig. 4 C). These data suggest that PEP expression in the hematopoietic compartment is necessary for augmented activation and proliferation in response to IFN-α signaling through the IFNAR.

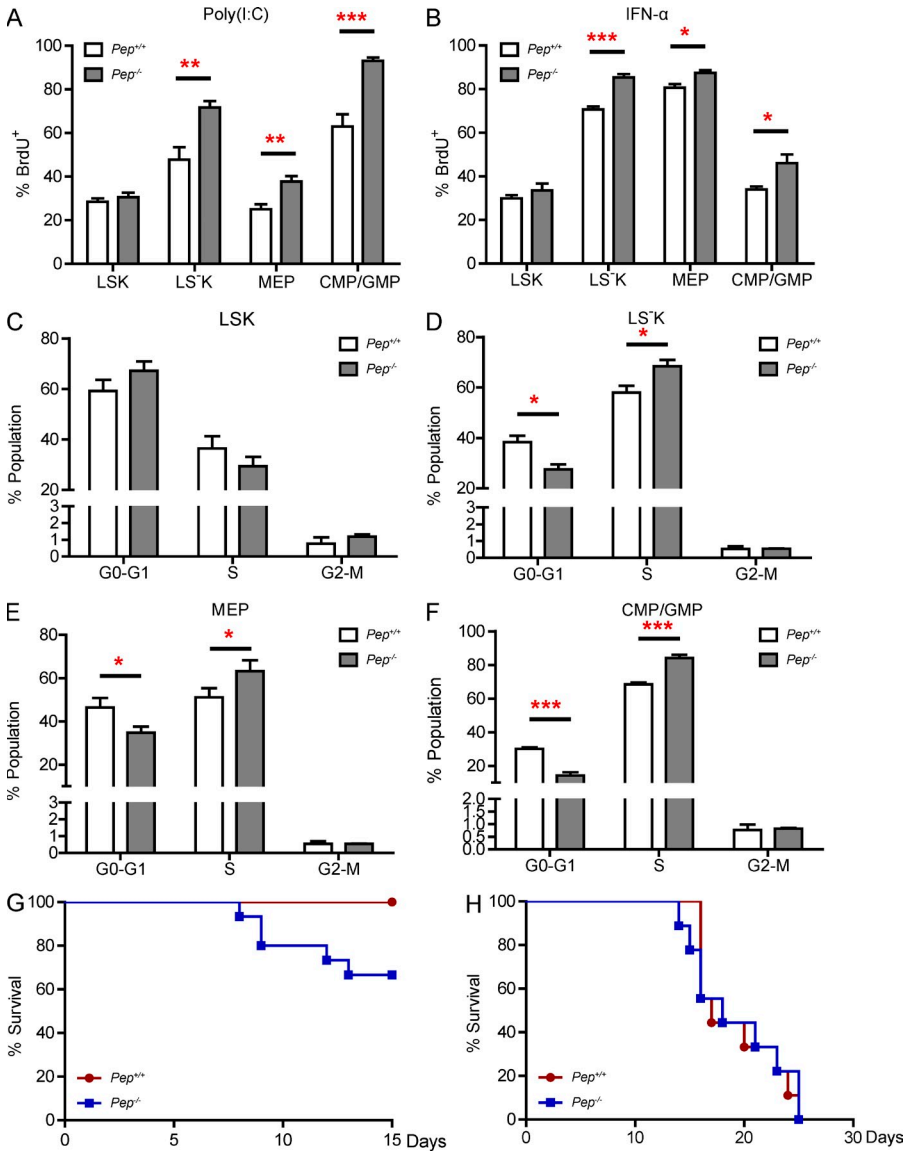

Figure 3. PEP negatively regulates progenitor proliferation after administration of poly(I:C) or IFN-α in vivo. (A and B) Analysis of BM progenitor proliferation with poly(I:C) (A) or IFN-α (B) administration *in vivo* in mice. *Pep*$^{+/+}$ and *Pep*$^{-/-}$ mice were injected i.p. with poly(I:C) (200 µg/mouse) for 23 h or infected with Ad5-IFN-α5 (10^7 PFU/mouse) for 36 h, followed by BrdU administration for 1 h. BrdU incorporation in BM progenitors was analyzed by FACS. Percentage of BrdU$^+$ cells in *Pep*$^{+/+}$ (open bar) and *Pep*$^{-/-}$ (grey bar) mice are depicted. $n = 4$ mice/genotype and data shown are representative of 3 independent experiments. (C–F) Analysis of cell cycle progression in poly(I:C) treated mice. *Pep*$^{+/+}$ (top) and *Pep*$^{-/-}$ (bottom) mice were treated with poly(I:C) for 23 h, followed by BrdU administration for 1 h. Cell cycle progression in BM progenitors was analyzed by FACS for G_0-G_1, S, and G_2-M in hematopoietic progenitors (LSK; C), LS$^-$K cells (D), MEP (E), and CMP/GMP (F) from *Pep*$^{+/+}$ (open bar) and *Pep*$^{-/-}$ (grey bar) mice. $n = 4$ mice/genotype and data shown are representative of 3 independent experiments. (G) *Pep*$^{+/+}$ ($n = 15$ mice, red) and *Pep*$^{-/-}$ ($n = 15$ mice, blue) mice were injected with poly(I:C) (200 µg/mouse). 48 h after poly(I:C) administration, mice were injected i.p. with 150 mg/kg 5-FU to determine intrinsic hematopoietic proliferation and exhaustion rates in vivo. Data are a compilation of three independent experiments. (H) *Pep*$^{+/+}$ ($n = 9$ mice, red) and *Pep*$^{-/-}$ ($n = 9$ mice, blue) mice were injected once weekly for 5 wk (i.p.) with 150 mg/kg 5-FU to deplete proliferating BM progenitors to induce BM failure. Data shown are representative of three independent experiments unless otherwise stated. Values in graphs represent means ± SEM. Statistical analysis was done by two-tailed paired Student's *t* test; *, $P < 0.05$; **, $P < 0.01$; ***, $P < 0.001$.

PEP is a negative regulator of IFNAR signaling in progenitor cells

Our data and that of others (Essers et al., 2009) suggest an intrinsic requirement for IFNAR signaling on progenitor cells during IFN-α–mediated disease and stress hematopoiesis. To determine the role of PEP in IFNAR signaling, lineage-depleted BM cells from *Pep*$^{+/+}$ and *Pep*$^{-/-}$ mice were treated with IFN-α and STAT1 phosphorylation was assessed by Western blot using an anti–phospho-specific STAT1 antibody. Addition of recombinant mouse IFN-α4 (rIFN-α4) to *Pep*$^{-/-}$ progenitors demonstrated a twofold increase in STAT1 phosphorylation on tyrosine 701 compared to *Pep*$^{+/+}$ progenitors (Fig. 5, A and B). Increased STAT1 phosphorylation was also observed using in vitro–generated *Pep*$^{-/-}$ myeloid progenitors (Fig. 5, C and D). To determine the downstream consequences of enhanced STAT phosphorylation in *Pep*$^{-/-}$ progenitor cells, we treated *Pep*$^{+/+}$ and *Pep*$^{-/-}$ mice with poly(I:C) for 16 h and sorted lineage-negative progenitor cells for transcriptome analysis. Consistent with increased phosphorylation and activation of STAT1, IFN-responsive genes *Isg15, Irf4, Mx1*, and *Osmr* were significantly up-regulated in *Pep*$^{-/-}$ compared to *Pep*$^{+/+}$ progenitor cells (Fig. 5 E and Table S1).

As PEP has been demonstrated to play a positive regulatory, rather than an inhibitory, function for TLR signaling in mouse macrophages (Wang et al., 2013), we analyzed the role of PEP in IFNAR signaling of BMDMs. Addition of rIFN-α4 to in vitro–differentiated BMDMs resulted in a time-dependent increase in STAT1 phosphorylation on tyrosine 701 that was further enhanced in *Pep*$^{-/-}$ BMDMs (Fig. 5, F-G). Whereas *Mx1* and *Irf4* mRNAs were not induced or below detection levels (CT > 35) in BMDMs, IFN-responsive genes *Irf8*, *Il7*, and *Prlr* mRNAs (Bovolenta et al., 1994; Martin et al.,

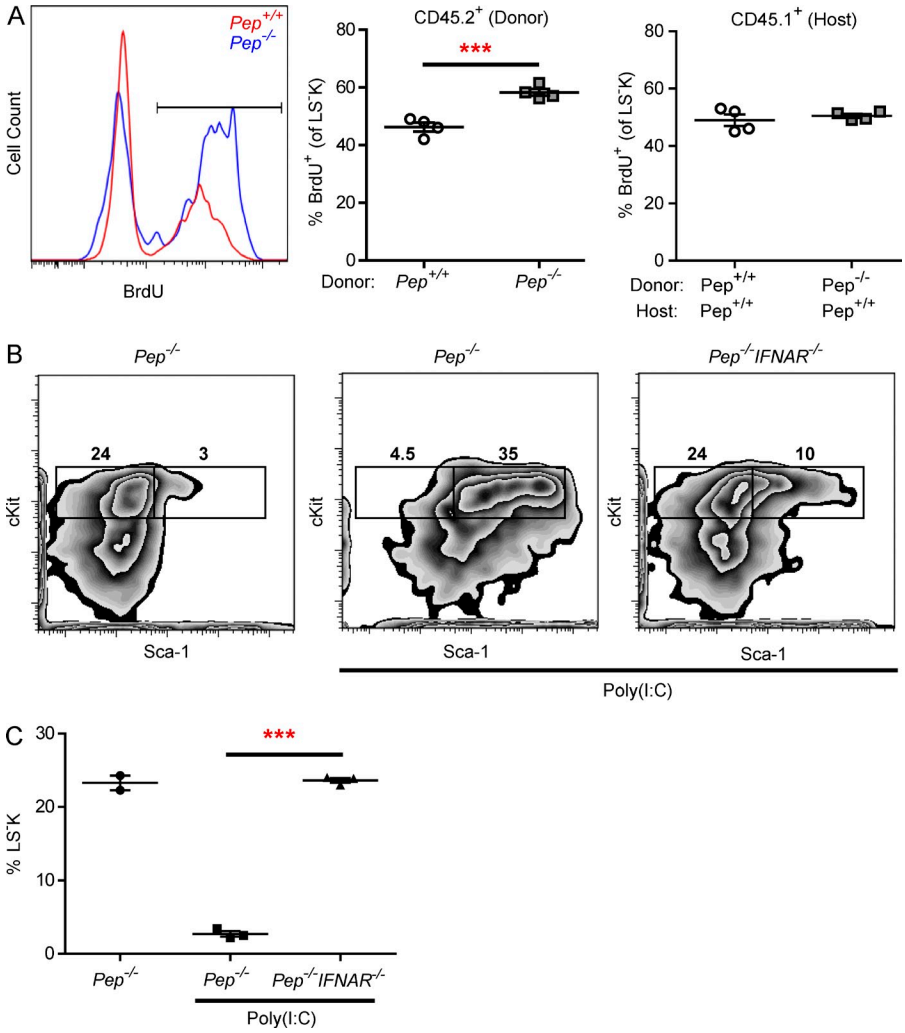

Figure 4. PEP and IFNAR are required for IFN-α–mediated progenitor proliferation. (A) Analysis of progenitor proliferation in BM chimeric mice. *Pep*$^{+/+}$ (red) and *Pep*$^{-/-}$ (blue) chimeric mice were treated with poly(I:C) for 23 h, followed by BrdU administration for 1 h. BrdU incorporation of BM progenitors was analyzed by FACS (left). Graphical representation (right) of BrdU incorporation in myeloid progenitors from donor (CD45.2$^+$; middle) *Pep*$^{+/+}$ (open circle) and *Pep*$^{-/-}$ (grey square) mice or myeloid progenitors from wild-type competitor (CD45.1$^+$) mice (right). $n = 4$ mice/genotype and data shown are representative of 3 independent experiments. (B) *Pep*$^{-/-}$ mice were untreated (left) and compared with *Pep*$^{-/-}$ (middle) or *Pep*$^{-/-}$*IFNAR*$^{-/-}$ (right) chimeric mice injected with poly(I:C). Sca-1 levels were assessed by FACS 24 h after poly(I:C) administration. A representative FACS plot is depicted here and quantitated in C. (C) Graphical representation of percentage of LS$^-$K lineage$^-$ BM from B in untreated (circle), poly(I:C)-treated *Pep*$^{-/-}$ (squares), or poly(I:C)-treated *Pep*$^{-/-}$*IFNAR*$^{-/-}$ (triangle) mice. $n = 4$ mice/genotype and data shown are representative of 3 independent experiments. Values in graphs represent means ± SEM. Statistical analysis was done by two-tailed paired Student's *t* test. ***, $P < 0.001$.

2004; Hou et al., 2015) were further augmented in *Pep*$^{-/-}$ compared to *Pep*$^{+/+}$ BMDMs after treatment with rIFN-α4 (Fig. 5 H and Table S2). Together, these data support a negative regulatory role for PEP on IFNAR signaling in HSCs and BMDMs.

To further explore the biochemical nature by which PEP regulates IFNAR signaling, we expressed PEP in 3T3 cells that are IFN-α responsive. 3T3 cells expressing transfected PEP demonstrated reduced STAT1 and STAT2 phosphorylation after rIFN-α4 stimulation compared to vector control cDNA-transfected cells (Fig. 6, A and B). The phosphatase activity of PEP was required for maximal reduction of STAT1 phosphorylation because expression of a catalytically inactive PEP(C227S) did not reduce STAT1 phosphorylation to the same extent as wild-type PEP (Fig. 6, C and D). Finally, we investigated whether PEP could co-localize with the IFNAR signaling complex. In 3T3 cells transfected with a *Pep* cDNA, PEP co-immunoprecipitated with multiple components of the IFNAR signaling complex, including JAK1, TYK2, SOCS1, IFNAR, and STAT1 (Fig. 6 E). Hence, PEP is physically positioned to regulate IFNAR signaling.

DISCUSSION

Our studies here provide a mechanistic basis by which PTPN22 and IFN-α pathways may cooperate to manifest cytopenias in SLE. *Pep*$^{-/-}$ mice treated with IFN-α or poly(I:C) demonstrate greater morbidity/mortality than treated *Pep*$^{+/+}$ mice. Although IFN-α has pleiotropic effects on both immune and nonimmune cells, our studies here reveal a novel role for PEP as a negative regulator of IFNAR signaling in hematopoietic progenitors. IFN-α induced a greater degree of activation as assessed by STAT1 phosphorylation and increased transcription of type I IFN-dependent genes and cell cycle entry of *Pep*$^{-/-}$ progenitors. In turn, these compound effects of IFN-α and PEP deficiency in mice result in severe anemia, thrombocytopenia, and neutropenia. IFN-α has recently emerged as an important regulator of hematopoiesis. IFN-α induces dormant HSCs to proliferate, and chronic IFN-α stimulation results in HSC dysfunction and exhaustion (Essers et al., 2009). Similarly, mice deficient in IRF2, a critical negative regulator of type I IFN signaling, have greater numbers of proliferating as opposed to dormant HSCs (Sato et al., 2009). As SLE patients with the PTPN22 at-risk variant have higher serum levels of

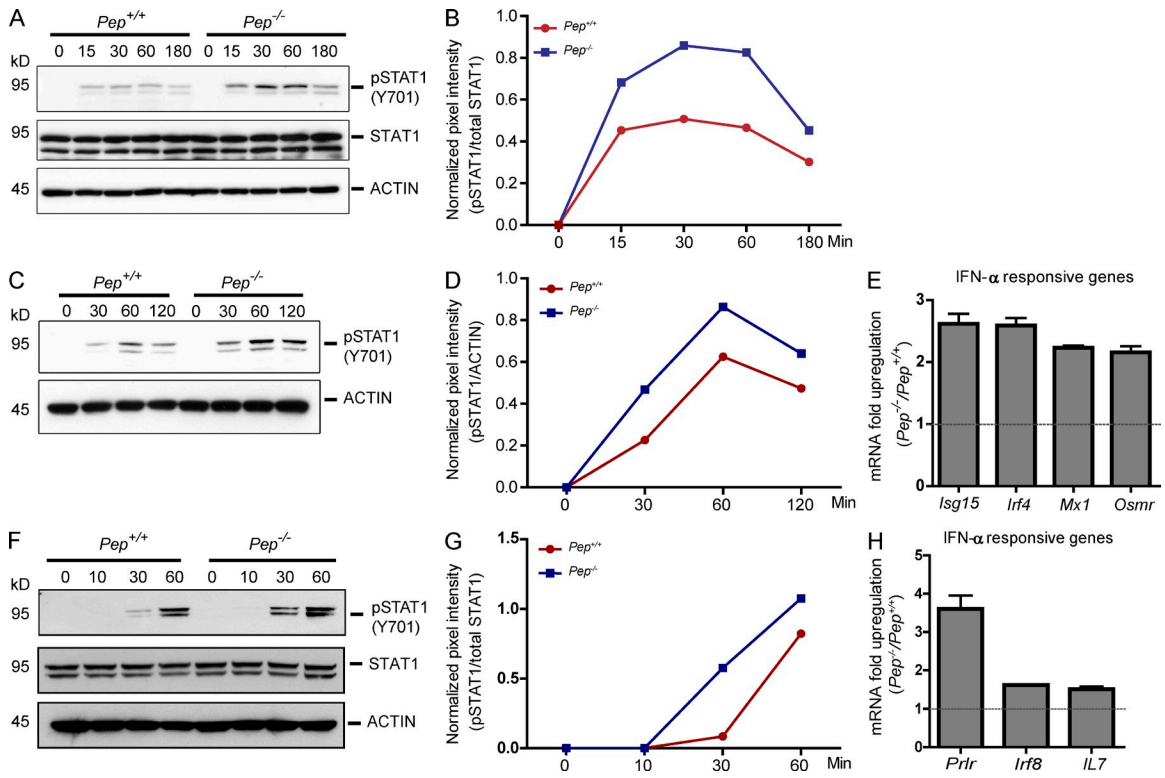

Figure 5. PEP is a negative regulator of IFNAR signaling. (A) Freshly isolated *Pep*$^{+/+}$ and *Pep*$^{-/-}$ lineage-depleted BM cells were stimulated with rIFN-α4 (2,000 U/ml) for the indicated times (minutes) and whole-cell extracts were isolated and analyzed for STAT1 activation (phosphorylated STAT1, top; total STAT1, middle) or ACTIN (bottom). (B) Relative band intensity by densitometry of pSTAT1 (α-isoform) normalized to relative band intensity of total STAT1 (α-isoform) from A is shown. (C) *Pep*$^{+/+}$ and *Pep*$^{-/-}$ lineage-depleted BM cells were expanded for 3-4 d in vitro with IL-3 (25 ng/ml), IL-6 (25 ng/ml), and SCF (50 ng/ml), treated with rIFN-α4 (2,000 U/ml) for the indicated times (minutes), and whole-cell extracts were analyzed by immunoblotting for phosphorylated STAT1 (top) and ACTIN (bottom). (D) Relative band intensity by densitometry of pSTAT1 (α-isoform) normalized to relative band intensity of ACTIN from C is shown. (E) *Pep*$^{+/+}$ and *Pep*$^{-/-}$ mice were injected with poly(I:C) for 16 h, and BM progenitors isolated and analyzed for expression of IFN-responsive genes by PCR array. Data are represented as fold up-regulation of *Pep*$^{-/-}$ relative to *Pep*$^{+/+}$ progenitor cells. Relative gene expression is expressed by $2\Delta C_t$ method. $P < 0.01$ for *Irf4*, *Mx1*, and *Osmr*; $P = 0.02$ for *Isg15*. (F) BMDMs from *Pep*$^{+/+}$ and *Pep*$^{-/-}$ mice were stimulated with rIFN-α4 (2,000 U/ml) for the indicated times and whole-cell extracts were isolated and analyzed for phosphorylated STAT1 (top), total STAT1 (middle), or ACTIN (bottom). (G) Relative band intensity by densitometry of pSTAT1 (α-isoform) normalized to relative band intensity of total STAT1 (α-isoform) from E is shown. (H) *Pep*$^{+/+}$ and *Pep*$^{-/-}$ BMDMs were stimulated with rIFN-α4 (2,000 U/ml) for 4 h and analyzed for expression of IFN-responsive genes by PCR array as described in E. Data shown (A, C, E, F, and H) are representative of three independent experiments. Values in graphs represent means ± SEM. Statistical analysis was done by two-tailed paired Student's *t* test. $P < 0.05$ for *Prlr*, *Irf8*, and *Il7*.

IFN-α (Kariuki et al, 2008), these synergistic effects of PTPN22 and IFN-α may provide an additional mechanistic basis for the BM dysfunction observed in SLE.

PEP was first demonstrated to regulate TCR signaling through association with CSK (Cloutier and Veillette, 1996), a PTK that represses SRC-family PTKs. Overexpression of PEP in T cells inhibits T cell functions (Cloutier and Veillette, 1999; Gjörloff-Wingren et al., 1999). Generation of *Pep*$^{-/-}$ mice on a nonautoimmune prone background (C57BL/6) revealed an essential function for PEP in effector/memory, but not naive, T cells. *Pep*$^{-/-}$ effector T cells demonstrate enhanced TCR signaling and, as *Pep*$^{-/-}$ mice age, they develop splenomegaly, spontaneous germinal center formation, and elevated serum IgG1, IgG2a, and IgE levels, though without any clinical manifestations of autoimmunity (Hasegawa et al., 2004). PEP also plays an important role in regulating weak agonist antigens in naive OT-1 TCR transgenic T cells on a *Rag1*$^{-/-}$ background or when competitively transferred into a profoundly lymphopenic environment by regulating TCR signaling and by modulating LFA-1–dependent inside-out signaling and adhesion (Salmond et al., 2014). Whereas autoantibody production was not observed in *Pep*$^{-/-}$ mice on a nonautoimmune prone strain (C57BL/6; Hasegawa et al., 2004), *Pep*$^{-/-}$ mice expressing a wedge CD45(E613R) mutation, that ablates dimerization-induced inhibition of CD45 phosphatase activity, on a C57BL/6 background developed systemic autoimmunity with autoantibody production, glomerulonephritis, and increased mortality greater than either single-mutant mice (Zikherman et al., 2009). Hence, PEP plays an important role in determining signaling thresholds in autoreactive T cells to maintain immunologic tolerance.

Studies of peripheral human T and B cells expressing the at-risk *PTPN22(C1858T)* allele suggested a gain-of-function phenotype with accumulation of circulating memory T cells,

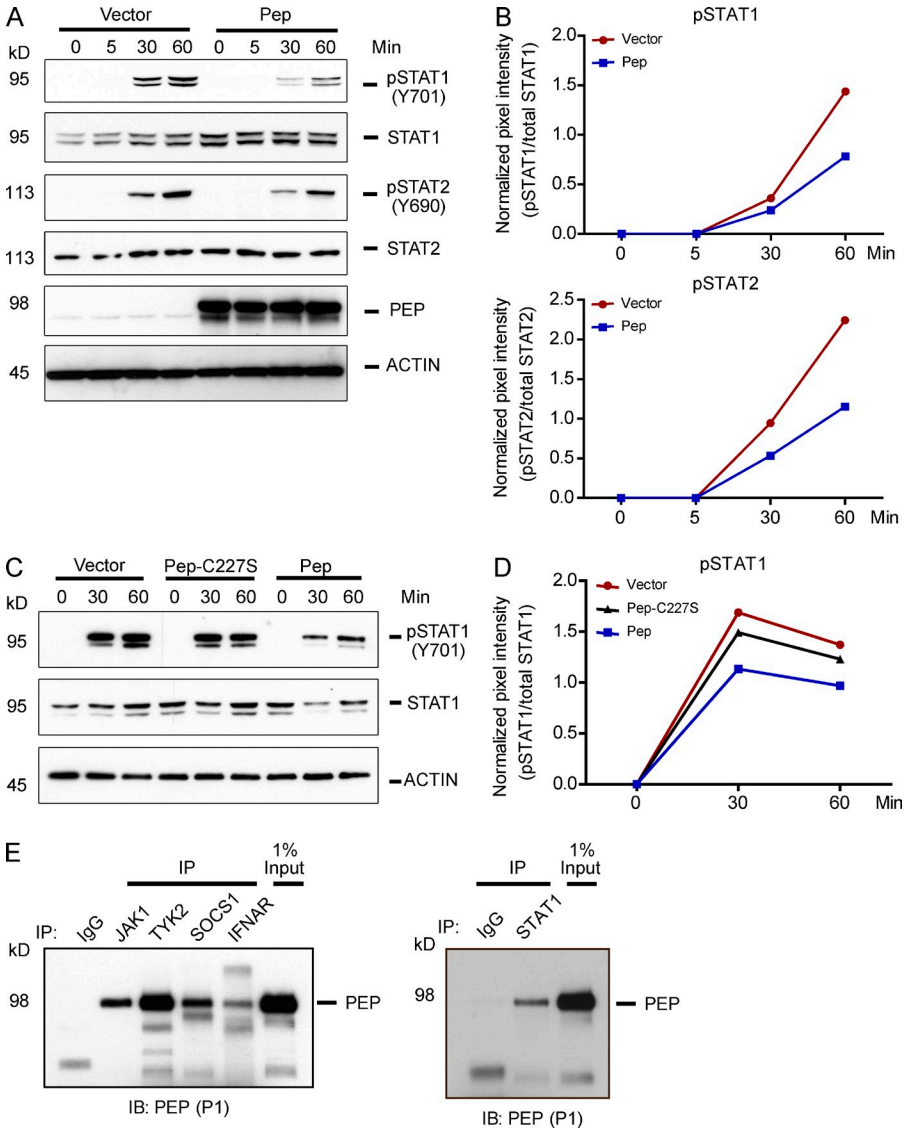

Figure 6. PEP interacts with the IFNAR signaling complex to negatively regulate IFNAR signaling. (A) 3T3 cells were transfected with vector or Pep cDNAs. 24 h after transfection, cells were stimulated with rIFN-α4 (2,000 U/ml) for indicated times and whole-cell extracts were analyzed by immunoblotting for phosphorylated STAT1 and total STAT1 (top), phosphorylated STAT2 and total STAT2 (middle), PEP, and ACTIN (bottom). (B) Relative band intensity by densitometry of pSTAT1 (α-isoform) and pSTAT2 normalized to relative band intensity of total STAT1 (α-isoform) and total STAT2, respectively, from A are shown. (C) 3T3 cells were transfected with vector, Pep-C227S, or Pep cDNAs. 24 h after transfection, cells were stimulated with rIFN-α4 (2,000 U/ml) for the indicated times and whole-cell extracts analyzed by immunoblotting for phosphorylated STAT1 and total STAT1 (top) and ACTIN (bottom) are shown. (D) Relative band intensity by densitometry of pSTAT1 (α-isoform) normalized to relative band intensity of total STAT1 (α-isoform) from C are shown. (E) 3T3 cells transfected with Pep or vector cDNAs were immunoprecipitated with anti-JAK1, -TYK2, -SOCS1, -IFNAR, -STAT1, or IgG control antibodies. Immunoprecipitates were resolved by SDS-PAGE and analyzed by Western blotting for PEP (P1 antibody). 1% cell lysates are shown for comparison. Data shown A, C, E, and F are representative of three independent experiments.

decreased numbers of circulating memory B cells, decreased TCR signaling, and impaired BCR signaling (Vang et al., 2005; Rieck et al., 2007; Arechiga et al., 2009). Further analysis of autoreactive B cells indicate that the *PTPN22(C1858T)* allelic variant interferes with deletion of autoreactive B cells (Menard et al., 2011; Habib et al., 2012).

Two groups have recently generated mice expressing the orthologous PEP(R619W) mutation that differ in their genetic backgrounds. In both cases, PEP(R619W) knock-in (KI) mice phenocopy *Pep*$^{-/-}$ mice with development of enhanced positive and negative T cell selection, enhanced TCR signaling, splenomegaly, lymphadenopathy, and spontaneous germinal center formation (Zhang et al., 2011; Dai et al., 2013). PEP(R619W) KI mice on a C57BL/6 background also exhibited enhanced antigen presentation by dendritic cells and modest increases in BCR signaling (Zhang et al., 2011). PEP(R619W) KI mice on a mixed C57BL/6J and 129/Sv genetic backgrounds differed from *Pep*$^{-/-}$ or PEP(R619W) KI C57BL6/J mice as they also demonstrated enhanced TCR signaling in naive T cells, altered B cell selection, and enhanced BCR signaling in mature B cells. Moreover, PEP(R619W) knock-in mice on a mixed background develop systemic autoimmunity with high-titer autoantibodies, vasculitis, and increased mortality (Dai et al., 2013).

The *PTPN22(C1858T)* polymorphism has now been described for a variety of autoimmune disorders. PTPN22/LYP associates with CSK in resting T cells and upon TCR activation, PTPN22 dissociates from CSK and translocates to lipid rafts where PTPN22/LYP can dephosphorylate and inactivate the TCR signalsome (Cloutier and Veillette, 1996; Vang et al., 2012). The PEP(R620W) variant alters the proline-rich region (P1) to disrupt its interaction with CSK (Begovich et al., 2004; Bottini et al., 2004). Although some have proposed that the *PTPN22(C1858T)* at risk variant can provide greater inhibition of antigen–receptor signaling due to its compromised ability to interact with and

be sequestered by CSK (Vang et al., 2012), another model suggests that the *PTPN22(C1858T)* at risk variant may differentially affect downstream effectors than *PTPN22* deficiency (Dai et al., 2013).

In addition to T and B cell antigen receptor signaling, PTPN22/PEP can play both positive and negative functions depending on receptor and cellular context. PEP plays a requisite function to dephosphorylate phosphoanandamide to generate anandamide, a lipid second messenger with anti-inflammatory effects produced by macrophages upon LPS induction (Liu et al., 2006). In the human THP-1 monocytic cell line, PTPN22 co-immunoprecipitates with SOCS1 and inhibits SOCS1 tyrosine phosphorylation to enhance IFN-γ signaling (Spalinger et al., 2013). In mouse macrophages, PEP interacts with TRAF3 and positively regulates type I IFN production after TLR stimulation. $Pep^{-/-}$ macrophages stimulated with LPS or poly(I:C) produce less IFN-β (Wang et al., 2013). Consistent with this requisite function for PEP in TLR signaling in macrophages, peripheral blood monocytes from *PTPN22(C1958T)* carriers for the at-risk allele demonstrated reduced STAT1 phosphorylation and reduced type 1 IFN-induced gene expression after LPS challenge (Wang et al, 2013). Contrary to the studies of Wang et al. (2013) using IFN-α and IFN-β, our studies demonstrate an inhibitory role of PEP in IFN-α4–mediated IFNAR signaling in BMDMs (Fig. 5, F–H). The basis of these differences is unclear and may relate to differences in IFN-α subtypes used as the potencies of the 12 IFN-αs differ (Hillyer et al., 2013), stimulation conditions, and/or differences in IFNAR signaling of IFN-α and IFN-β (de Weerd et al., 2013).

Our studies here support an inhibitory function for PEP in IFNAR function in hematopoietic precursors and BMDMs. PEP phosphatase activity is required for optimal IFNAR regulation, though it is likely that additional noncatalytic scaffolding domains can also contribute to PEP function. Additionally, as PEP can be coimmunoprecipitated with the IFNAR signaling complex, PEP is appropriately positioned to down-regulate IFN-α–induced signaling through JAK1, TYK2, SOCS, STATs, and other IFNAR regulators. Additional biochemical studies will be required to better define the molecular nature by which PEP regulates IFNAR signaling.

A similar duality of function has also been demonstrated for the CD45 PTPase. Whereas CD45 is required for T and B cell development, as well as T and B cell antigen receptor signaling (Hermiston et al., 2003), CD45 plays an inhibitory role in cytokine, IFNAR, and α5β1 integrin-mediated signaling (Penninger et al., 2001). CD45 interacts with JAKs and down-regulates IL-3 and cKit-mediated proliferation of BM-derived mast cell lines, erythropoietin-mediated erythropoiesis, IL-3–mediated differentiation of BM precursors to neutrophil/macrophage colonies, and IFN-regulated antiviral responses (Irie-Sasaki et al., 2001). In addition, CD45 is required for α5β1 integrin-mediated adhesion to fibronectin, an activity dependent on both CD45 phosphatase activity and CD45 association with CD45-associated protein (Shenoi et al., 1999).

In summary, our study provides insights by which PEP and IFN-α might cooperate to give rise to dysfunctional hematopoiesis. As a consequence of dysregulated IFN-α expression in SLE, patients carrying the *PTPN22(C1858T)* risk variant may have enhanced IFN-α–mediated JAK–STAT signaling in HSCs to exhaust their precursor pool that manifest in hematologic abnormalities in SLE.

MATERIALS AND METHODS

Mice. B6.SJL-*Ptprc*^{a} *Pepc*^{b}/BoyJ mice were purchased from The Jackson Laboratory. $Pep^{-/-}$ mouse generation was previously described (Hasegawa et al., 2004). $IFNAR^{-/-}$ mice were purchased from The Jackson Laboratory for breeding with $Pep^{+/+}$ and $Pep^{-/-}$ mice. All mice were maintained under specific pathogen–free conditions unless otherwise noted. Poly(I:C) (LMW) was purchased from InvivoGen, and mice were administered 200 μg/mouse i.p. for the indicated times. 5-FU was purchased from APP Pharmaceuticals. For 5-FU studies, mice were administered 200 μg poly(I:C) i.p. and, 48 h later, injected with a single dose of 5-FU (150 mg/kg), or mice were injected once weekly for the length of the experiment. All animal experimentation protocols were approved by the Laboratory Animal Resources Committee at Genentech, Inc. (South San Francisco, CA).

BM chimeras. 8-wk-old ($CD45.1^+$) $Pep^{+/+}$ (B6.SJL-*Ptprc*^{a} *Pepc*^{b}/BoyJ) mice were lethally irradiated (2 doses of 500 cGy with 137Cs γ-irradiator) at 3-h intervals and ∼3 h before injection. BM from $Pep^{+/+}$ ($CD45.1^+$) mice were isolated and mixed at a 1:1 ratio with either $Pep^{+/+}$ or $Pep^{-/-}$ ($CD45.2^+$) or $Pep^{-/-}IFNAR^{-/-}$ ($CD45.2^+$) BM in Dulbecco's Modification of Eagle's Medium. Irradiated mice ($CD45.1^+$) were injected in the lateral tail vein with approximately 1×10^6 total BM cells. All irradiated mice were given antibiotic-supplemented water (1.1 g/l neomycin and 110 mg/l polymycin B; Sigma-Aldrich) for 2 wk.

Adenoviral and recombinant IFN-α. Mouse IFN-α5 was cloned into a pShuttleX vector and transferred into Ad5 viral vector by the Baylor College of Medicine Vector Development Lab (VDL). Ad5-IFN-α and Ad5-LacZ control viruses were purified on CsCl gradients and titered per VDL specification. Virus was administered by i.v. injection into 16-20-wk-old female mice. For in vitro experiments, recombinant mouse IFN-α4 (rIFN-α4) was purchased from PBL Assay Sciences.

Cell preparations. BM-derived myeloid progenitor cells were generated from hematopoietic progenitor cells isolated from BM using a Miltenyi MACS lineage depletion kit. Cells were stimulated for 3 d in IL-3 (25 ng/ml), IL-6 (25 ng/ml), and SCF (50 ng/ml), washed, and stimulated for indicated times with rIFN-α4 (2,000 U/ml, PBL Assay Science). BMDMs were differentiated by incubating total BM cells in 15-cm tissue culture plates with recombinant M-CSF (100 ng/ml; Genentech) in DMEM for 7-10 d. M-CSF (100 ng/ml) was replenished every 3 d during culturing. BMDMs were plated overnight in M-CSF, rested for 4 h and stimulated for the indicated times with rIFN-α4 (2,000 U/ml; PBL Assay Science). For cell transfection experiments, 3T3 cells were transfected using Lipofectamine LTX with plus reagent (Life Technologies) according to manufacturer's instruction.

Complete blood count. Blood was collected from IFN-α treated $Pep^{+/+}$ and $Pep^{-/-}$ mice in Microtainer tubes (BD) containing EDTA. Cell counts were analyzed on a XT-V Automated Hematology Analyzer (Sysmex).

Renal histologic evaluation. Kidneys from IFN-α administered $Pep^{+/+}$ ($n = 5$) and $Pep^{-/-}$ ($n = 3$) mice were fixed in 10% neutral buffer formalin, processed, and embedded in paraffin for sectioning. ∼3-μm sections were de-paraffinized and stained with hematoxylin and eosin or Periodic acid-Schiff (PAS). Renal lesions were scored on arbitrary severity scales from 0 to 3 for each of the features: glomerulopathy, interstitial nephritis, and arteritis. Proteinuria was evaluated in urine collected weekly. Urine protein levels

were scored with Multistix 10 SG (Siemens) dipsticks on a Clinitek Status Analyzer (Siemens). Protein levels are scored as 1 (30 mg/dl), 2 (100 mg/dl), or 3 (>300 mg/dl).

ANA and BAFF ELISA. Serum IgG antinuclear antibodies (ANA) were measured using an Alpha Diagnostic International per the manufacturer's instruction. BAFF detection was determined using an anti-BAFF soluble mouse detection kit (Enzo Life Sciences) per manufacturer's instruction.

Flow cytometry. Single-cell suspensions from spleen, blood, BM, or BALF were washed in PBS containing 5 mM ethylenediaminetetraacetic acid and 0.5% BSA. Cells were incubated for 15 min with Fc receptor block (clone 2.4G2; BD) before antibody staining. The following antibodies were used for FACS staining and sorting: biotinylated antibodies for lineage-negative staining-biotin lineage staining cocktail includes CD3, B220, GR-1, CD11b, and Ter119, as well as NK1.1, CD11c, and DX-5 (BD), were added to the staining cocktail; CD45.2 (104), cKit (2B8), and CD34 (Ram34) were purchased from BD; CD16/32 (93), Sca-1 (D7), and CD135 (A2F10) were purchased from eBioscience; CD45.1 (A20), CD48 (HM48-1), and CD150 (TC15-12F12.2) were purchased from BioLegend. Aqua Fluorescent reactive dye (Life Technologies) was used to discriminate viable from dead cells. Intracellular BrdU and 7AAD for cell cycle analysis using the FITC BrdU Flow kit (BD) was performed per the manufacturer's protocol. Flow cytometry data was analyzed using FlowJo software (Tree Star).

Immunoprecipitation. 3T3 cells were lysed in 100 mM Tris buffer containing 1% Triton X-100, protease inhibitor, phosphatase inhibitor, NaF (10 mM), and PMSF (1 mM) for 30 minutes with rotation at 4°C, and cleared by centrifugation at 12,000 rpm for 5 min. Antibodies used for immunoprecipitation included IFNAR1 (Santa Cruz Biotechnology, Inc.), STAT1 (Cell Signaling Technology), SOCS1 (Abcam), TYK2 (Abcam), and JAK1 (Santa Cruz Biotechnology, Inc.). Protein/antibody conjugates were precipitated with protein A Dynabeads (Life Technologies) and washed four times in lysis buffer. Beads were boiled in LDS buffer (Life Technologies) and loaded on 8% Tris-glycine gel (Novex; Life Technologies).

Western blot analysis. Whole-cell lysates were generated with RIPA lysis buffer (Thermo Fisher Scientific) with protease and phosphatase inhibitors, DTT (1 mM), NaF (10 mM), and PMSF (1 mM). Total protein from each fraction was determined by BSA quantification method (Thermo Fisher Scientific). Cell lysates were loaded on a NuPAGE 4-12% Bis-Tris gel (Life Technologies) and transferred to PVDF membrane using an iBlot Gel transfer device (Invitrogen). Membranes were blocked with 5% milk and 0.2% Tween in PBS. Antibodies specific for ACTIN, STAT1, and STAT2 were purchased from Cell Signaling Technology. Antibodies for pSTAT1, pSTAT2, SOCS1, and TYK2 were purchased from Abcam. Anti-PEP (P1) antisera to detect PEP by Western blotting have been previously described (Hasegawa et al., 2004). All antibodies were diluted in blocking buffer and incubated overnight at 4°C. Secondary antibodies included HRP (Millipore)-conjugated goat anti–rabbit or goat anti–mouse antibodies in conjunction with Amersham ECL prime Western blotting detection reagent (GE Healthcare) to visualize bands using x-ray film (Kodak). Bands were measured by densitometry analysis using ImageJ analysis software (National Institutes of Health).

Mouse IFN and receptor PCR array. RNA was prepared using RNeasy Mini Plus kits (QIAGEN) and reverse-transcribed with RT^2 First Strand kit (QIAGEN), in accordance with the manufacturer's instructions. Mouse IFN and receptor PCR Array was performed according to manufacturer's instruction (QIAGEN). PCR array (PAMM-064ZE) was performed and gene expression measured on a 7900HT Fast Real-Time PCR System (Applied Biosystems).

Online supplemental material. Table S1 shows increased IFN-responsive gene transcription in *Pep*$^{-/-}$ BM progenitors. Table S2 shows IFN-responsive genes in BMDMs. Online supplemental material is available at http://www.jem.org/cgi/content/full/jem.20142130/DC1.

All authors are or were (D.A. Holmes and H.R.C. Smith) employees of Genentech, Inc. The authors declare no additional competing financial interests.

Author contributions: D.A. Holmes designed experiments, generated, and interpreted data, and prepared the manuscript. Q. Ou and Q. Gong designed, generated, and interpreted data presented in Fig. 5 (F–H) and Table S2. H.R.C. Smith contributed to the initial design and execution of the experiments represented in Fig. 1. A.C. Chan designed experiments, interpreted data, and prepared the manuscript. E. Suto and W.P. Lee performed injections of Ad5 virus. P. Caplazi performed pathology analysis.

Submitted: 12 November 2014
Accepted: 15 May 2015

REFERENCES

Adam, C., Y. Thoua, P. Ronco, P. Verroust, M. Tovey, and L. Morel-Maroger. 1980. The effect of exogenous interferon: acceleration of autoimmune and renal diseases in (NZB/W) F1 mice. *Clin. Exp. Immunol.* 40:373–382.

Agrawal, H., N. Jacob, E. Carreras, S. Bajana, C. Putterman, S. Turner, B. Neas, A. Mathian, M.N. Koss, W. Stohl, et al. 2009. Deficiency of type I IFN receptor in lupus-prone New Zealand mixed 2328 mice decreases dendritic cell numbers and activation and protects from disease. *J. Immunol.* 183:6021–6029. http://dx.doi.org/10.4049/jimmunol.0803872

Arechiga, A.F., T. Habib, Y. He, X. Zhang, Z.Y. Zhang, A. Funk, and J.H. Buckner. 2009. Cutting edge: the PTPN22 allelic variant associated with autoimmunity impairs B cell signaling. *J. Immunol.* 182:3343–3347. http://dx.doi.org/10.4049/jimmunol.0713370

Baccala, R., R. Gonzalez-Quintial, R.D. Schreiber, B.R. Lawson, D.H. Kono, and A.N. Theofilopoulos. 2012. Anti-IFN-α/β receptor antibody treatment ameliorates disease in lupus-predisposed mice. *J. Immunol.* 189:5976–5984. http://dx.doi.org/10.4049/jimmunol.1201477

Baechler, E.C., F.M. Batliwalla, G. Karypis, P.M. Gaffney, W.A. Ortmann, K.J. Espe, K.B. Shark, W.J. Grande, K.M. Hughes, V. Kapur, et al. 2003. Interferon-inducible gene expression signature in peripheral blood cells of patients with severe lupus. *Proc. Natl. Acad. Sci. USA.* 100:2610–2615. http://dx.doi.org/10.1073/pnas.0337679100

Bashal, F. 2013. Hematological disorders in patients with systemic lupus erythematosus. *Open Rheumatol J.* 7:87–95. http://dx.doi.org/10.2174/1874312901307010087

Begovich, A.B., V.E. Carlton, L.A. Honigberg, S.J. Schrodi, A.P. Chokkalingam, H.C. Alexander, K.G. Ardlie, Q. Huang, A.M. Smith, J.M. Spoerke, et al. 2004. A missense single-nucleotide polymorphism in a gene encoding a protein tyrosine phosphatase (PTPN22) is associated with rheumatoid arthritis. *Am. J. Hum. Genet.* 75:330–337. http://dx.doi.org/10.1086/422827

Bengtsson, A.A., G. Sturfelt, L. Truedsson, J. Blomberg, G. Alm, H. Vallin, and L. Rönnblom. 2000. Activation of type I interferon system in systemic lupus erythematosus correlates with disease activity but not with antiretroviral antibodies. *Lupus.* 9:664–671. http://dx.doi.org/10.1191/096120300674499064

Bottini, N., and E.J. Peterson. 2014. Tyrosine phosphatase PTPN22: multifunctional regulator of immune signaling, development, and disease. *Annu. Rev. Immunol.* 32:83–119. http://dx.doi.org/10.1146/annurev-immunol-032713-120249

Bottini, N., L. Musumeci, A. Alonso, S. Rahmouni, K. Nika, M. Rostamkhani, J. MacMurray, G.F. Meloni, P. Lucarelli, M. Pellecchia, et al. 2004. A functional variant of lymphoid tyrosine phosphatase is associated with type I diabetes. *Nat. Genet.* 36:337–338. http://dx.doi.org/10.1038/ng1323

Bovolenta, C., P.H. Driggers, M.S. Marks, J.A. Medin, A.D. Politis, S.N. Vogel, D.E. Levy, K. Sakaguchi, E. Appella, J.E. Coligan, et al. 1994. Molecular interactions between interferon consensus sequence binding protein and members of the interferon regulatory factor family. *Proc. Natl. Acad. Sci. USA.* 91:5046–5050.

Butler, W.T., J.T. Sharp, R.D. Rossen, M.D. Lidsky, K.K. Mittal, and D.A. Gard. 1972. Relationship of the clinical course of systemic lupus erythematosus

to the presence of circulating lymphocytotoxic antibodies. *Arthritis Rheum.* 15:251–258. http://dx.doi.org/10.1002/art.1780150302

Carpenter, D.F., A.D. Steinberg, P.H. Schur, and N. Talal. 1970. The pathogenesis of autoimmunity in New Zealand mice. II. Acceleration of glomerulonephritis by polyinosinic polycytidylic acid. *Lab. Invest.* 23:628–634.

Chung, S.A., K.E. Taylor, R.R. Graham, J. Nititham, A.T. Lee, W.A. Ortmann, C.O. Jacob, M.E. Alarcón-Riquelme, B.P. Tsao, J.B. Harley, et al. SLEGEN. 2011. Differential genetic associations for systemic lupus erythematosus based on anti-dsDNA autoantibody production. *PLoS Genet.* 7:e1001323. http://dx.doi.org/10.1371/journal.pgen.1001323

Cloutier, J.F., and A. Veillette. 1996. Association of inhibitory tyrosine protein kinase p50csk with protein tyrosine phosphatase PEP in T cells and other hemopoietic cells. *EMBO J.* 15:4909–4918.

Cloutier, J.F., and A. Veillette. 1999. Cooperative inhibition of T-cell antigen receptor signaling by a complex between a kinase and a phosphatase. *J. Exp. Med.* 189:111–121.

Cui, Y., Y. Sheng, and X. Zhang. 2013. Genetic susceptibility to SLE: recent progress from GWAS. *J. Autoimmun.* 41:25–33.

Cunninghame Graham, D.S., D.L. Morris, T.R. Bhangale, L.A. Criswell, A.C. Syvänen, L. Rönnblom, T.W. Behrens, R.R. Graham, and T.J. Vyse. 2011. Association of NCF2, IKZF1, IRF8, IFIH1, and TYK2 with systemic lupus erythematosus. *PLoS Genet.* 7:e1002341.

Dai, X., R.G. James, T. Habib, S. Singh, S. Jackson, S. Khim, R.T. Moon, D. Liggitt, A. Wolf-Yadlin, J.H. Buckner, and D.J. Rawlings. 2013. A disease-associated PTPN22 variant promotes systemic autoimmunity in murine models. *J. Clin. Invest.* 123:2024–2036. http://dx.doi.org/10.1172/JCI66963

de Weerd, N.A., J.P. Vivian, T.K. Nguyen, N.E. Mangan, J.A. Gould, S.J. Braniff, L. Zaker-Tabrizi, K.Y. Fung, S.C. Forster, T. Beddoe, et al. 2013. Structural basis of a unique interferon-β signaling axis mediated via the receptor IFNAR1. *Nat. Immunol.* 14:901–907. http://dx.doi.org/10.1038/ni.2667

Essers, M.A., S. Offner, W.E. Blanco-Bose, Z. Waibler, U. Kalinke, M.A. Duchosal, and A. Trumpp. 2009. IFNalpha activates dormant haematopoietic stem cells in vivo. *Nature.* 458:904–908. http://dx.doi.org/10.1038/nature07815

García-Valladares, I., Y. Atisha-Fregoso, Y. Richaud-Patin, J. Jakez-Ocampo, E. Soto-Vega, D. Elías-López, E. Carrillo-Maravilla, J. Cabiedes, A. Ruiz-Argüelles, and L. Llorente. 2006. Diminished expression of complement regulatory proteins (CD55 and CD59) in lymphocytes from systemic lupus erythematosus patients with lymphopenia. *Lupus.* 15:600–605. http://dx.doi.org/10.1177/0961203306071916

Gateva, V., J.K. Sandling, G. Hom, K.E. Taylor, S.A. Chung, X. Sun, W. Ortmann, R. Kosoy, R.C. Ferreira, G. Nordmark, et al. 2009. A large-scale replication study identifies TNIP1, PRDM1, JAZF1, UHRF1BP1 and IL10 as risk loci for systemic lupus erythematosus. *Nat. Genet.* 41:1228–1233. http://dx.doi.org/10.1038/ng.468

Gjörloff-Wingren, A., M. Saxena, S. Williams, D. Hammi, and T. Mustelin. 1999. Characterization of TCR-induced receptor-proximal signaling events negatively regulated by the protein tyrosine phosphatase PEP. *Eur. J. Immunol.* 29:3845–3854. http://dx.doi.org/10.1002/(SICI)1521-4141(199912)29:12<3845::AID-IMMU3845>3.0.CO;2-U

Habib, T., A. Funk, M. Rieck, A. Brahmandam, X. Dai, A.K. Panigrahi, E.T. Luning Prak, A. Meyer-Bahlburg, S. Sanda, C. Greenbaum, et al. 2012. Altered B cell homeostasis is associated with type I diabetes and carriers of the PTPN22 allelic variant. *J. Immunol.* 188:487–496. http://dx.doi.org/10.4049/jimmunol.1102176

Hall, J.C., and A. Rosen. 2010. Type I interferons: crucial participants in disease amplification in autoimmunity. *Nat Rev Rheumatol.* 6:40–49. http://dx.doi.org/10.1038/nrrheum.2009.237

Han, J.W., H.F. Zheng, Y. Cui, L.D. Sun, D.Q. Ye, Z. Hu, J.H. Xu, Z.M. Cai, W. Huang, G.P. Zhao, et al. 2009. Genome-wide association study in a Chinese Han population identifies nine new susceptibility loci for systemic lupus erythematosus. *Nat. Genet.* 41:1234–1237. http://dx.doi.org/10.1038/ng.472

Harley, J.B., M.E. Alarcón-Riquelme, L.A. Criswell, C.O. Jacob, R.P. Kimberly, K.L. Moser, B.P. Tsao, T.J. Vyse, C.D. Langefeld, S.K. Nath, et al. International Consortium for Systemic Lupus Erythematosus Genetics (SLEGEN). 2008. Genome-wide association scan in women with systemic lupus erythematosus identifies susceptibility variants in ITGAM, PXK, KIAA1542 and other loci. *Nat. Genet.* 40:204–210. http://dx.doi.org/10.1038/ng.81

Hasegawa, K., F. Martin, G. Huang, D. Tumas, L. Diehl, and A.C. Chan. 2004. PEST domain-enriched tyrosine phosphatase (PEP) regulation of effector/memory T cells. *Science.* 303:685–689. http://dx.doi.org/10.1126/science.1092138

Heremans, H., A. Billiau, A. Colombatti, J. Hilgers, and P. de Somer. 1978. Interferon treatment of NZB mice: accelerated progression of autoimmune disease. *Infect. Immun.* 21:925–930.

Hermiston, M.L., Z. Xu, and A. Weiss. 2003. CD45: a critical regulator of signaling thresholds in immune cells. *Annu. Rev. Immunol.* 21:107–137. http://dx.doi.org/10.1146/annurev.immunol.21.120601.140946

Hillyer, P., N. Raviv, D.M. Gold, D. Dougherty, J. Liu, T.R. Johnson, B.S. Graham, and R.L. Rabin. 2013. Subtypes of type I IFN differentially enhance cytokine expression by suboptimally stimulated CD4(+) T cells. *Eur. J. Immunol.* 43:3197–3208. http://dx.doi.org/10.1002/eji.201243288

Ho, V., A. Mclean, and S. Terry. 2008. Severe systemic lupus erythematosus induced by antiviral treatment for hepatitis C. *J. Clin. Rheumatol.* 14:166–168. http://dx.doi.org/10.1097/RHU.0b013e3181775e80

Hom, G., R.R. Graham, B. Modrek, K.E. Taylor, W. Ortmann, S. Garnier, A.T. Lee, S.A. Chung, R.C. Ferreira, P.V. Pant, et al. 2008. Association of systemic lupus erythematosus with C8orf13-BLK and ITGAM-ITGAX. *N. Engl. J. Med.* 358:900–909.

Hou, L., Z. Jie, Y. Liang, M. Desai, L. Soong, and J. Sun. 2015. Type 1 interferon -induced IL-7 maintains CD8+ T-cell responses and homeostasis by suppressing PD-1 expression in viral hepatitis. *Cell. Mol. Immunol.* 12:213–221. http://dx.doi.org/10.1038/cmi.2014.49

Irie-Sasaki, J., T. Sasaki, W. Matsumoto, A. Opavsky, M. Cheng, G. Welstead, E. Griffiths, C. Krawczyk, C.D. Richardson, K. Aitken, et al. 2001. CD45 is a JAK phosphatase and negatively regulates cytokine receptor signalling. *Nature.* 409:349–354. http://dx.doi.org/10.1038/35053086

Jørgensen, T.N., E. Roper, J.M. Thurman, P. Marrack, and B.L. Kotzin. 2007. Type I interferon signaling is involved in the spontaneous development of lupus-like disease in B6.Nba2 and (B6.Nba2 x NZW)F(1) mice. *Genes Immun.* 8:653–662. http://dx.doi.org/10.1038/sj.gene.6364430

Kalunian, K.C., J.T. Merrill, R. Maciuca, J.M. McBride, M.J. Townsend, X. Wei, J.C. Davis, and W.P. Kennedy. 2015. A Phase II study of the efficacy and safety of rotalizumab (rhuMAb interferon-a) in systemic lupus erythematosus (ROSE). *Ann. Rheum. Dis.* http://dx.doi.org/10.1136/annrheumdis-2014-206090

Kariuki, S.N., M.K. Crow, and T.B. Niewold. 2008. The PTPN22 C1858T polymorphism is associated with skewing of cytokine profiles toward high interferon-alpha activity and low tumor necrosis factor alpha levels in patients with lupus. *Arthritis Rheum.* 58:2818–2823.

Kyogoku, C., C.D. Langefeld, W.A. Ortmann, A. Lee, S. Selby, V.E. Carlton, M. Chang, P. Ramos, E.C. Baechler, F.M. Batliwalla, et al. 2004. Genetic association of the R620W polymorphism of protein tyrosine phosphatase PTPN22 with human SLE. *Am. J. Hum. Genet.* 75:504–507. http://dx.doi.org/10.1086/423790

Lessard, C.J., I. Adrianto, J.A. Ice, G.B. Wiley, J.A. Kelly, S.B. Glenn, A.J. Adler, H. Li, A. Rasmussen, A.H. Williams, et al. GENLES Network. 2012. Identification of IRF8, TMEM39A, and IKZF3-ZPBP2 as susceptibility loci for systemic lupus erythematosus in a large-scale multiracial replication study. *Am. J. Hum. Genet.* 90:648–660. http://dx.doi.org/10.1016/j.ajhg.2012.02.023

Liu, J., L. Wang, J. Harvey-White, D. Osei-Hyiaman, R. Razdan, Q. Gong, A.C. Chan, Z. Zhou, B.X. Huang, H.Y. Kim, and G. Kunos. 2006. A biosynthetic pathway for anandamide. *Proc. Natl. Acad. Sci. USA.* 103:13345–13350. http://dx.doi.org/10.1073/pnas.0601832103

Martin, C., L. Pessemesse, M.P. De La Llosa-Hermier, J. Martal, J. Djiane, and M. Charlier. 2004. Interferon-tau upregulates prolactin receptor mRNA in the ovine endometrium during the peri-implantation period. *Reproduction.* 128:99–105. http://dx.doi.org/10.1530/rep.1.00158

Mathian, A., A. Weinberg, M. Gallegos, J. Banchereau, and S. Koutouzov. 2005. IFN-alpha induces early lethal lupus in preautoimmune (New Zealand

Black x New Zealand White) F1 but not in BALB/c mice. *J. Immunol.* 174:2499–2506. http://dx.doi.org/10.4049/jimmunol.174.5.2499

Menard, L., D. Saadoun, I. Isnardi, Y.S. Ng, G. Meyers, C. Massad, C. Price, C. Abraham, R. Motaghedi, J.H. Buckner, et al. 2011. The PTPN22 allele encoding an R620W variant interferes with the removal of developing autoreactive B cells in humans. *J. Clin. Invest.* 121:3635–3644. http://dx.doi.org/10.1172/JCI45790

Mittal, K.K., R.D. Rossen, J.T. Sharp, M.D. Lidsky, and W.T. Butler. 1970. Lymphocyte cytotoxic antibodies in systemic lupus erythematosus. *Nature.* 225:1255–1256. http://dx.doi.org/10.1038/2251255a0

Penninger, J.M., J. Irie-Sasaki, T. Sasaki, and A.J. Oliveira-dos-Santos. 2001. CD45: new jobs for an old acquaintance. *Nat. Immunol.* 2:389–396.

Rawlings, D.J., X. Dai, and J.H. Buckner. 2015. The role of PTPN22 risk variant in the development of autoimmunity: finding common ground between mouse and human. *J. Immunol.* 194:2977–2984. http://dx.doi.org/10.4049/jimmunol.1403034

Rhee, I., and A. Veillette. 2012. Protein tyrosine phosphatases in lymphocyte activation and autoimmunity. *Nat. Immunol.* 13:439–447. http://dx.doi.org/10.1038/ni.2246

Rieck, M., A. Arechiga, S. Onengut-Gumuscu, C. Greenbaum, P. Concannon, and J.H. Buckner. 2007. Genetic variation in PTPN22 corresponds to altered function of T and B lymphocytes. *J. Immunol.* 179:4704–4710. http://dx.doi.org/10.4049/jimmunol.179.7.4704

Salmond, R.J., R.J. Brownlie, V.L. Morrison, and R. Zamoyska. 2014. The tyrosine phosphatase PTPN22 discriminates weak self peptides from strong agonist TCR signals. *Nat. Immunol.* 15:875–883. http://dx.doi.org/10.1038/ni.2958

Santiago-Raber, M.L., R. Baccala, K.M. Haraldsson, D. Choubey, T.A. Stewart, D.H. Kono, and A.N. Theofilopoulos. 2003. Type-I interferon receptor deficiency reduces lupus-like disease in NZB mice. *J. Exp. Med.* 197:777–788. http://dx.doi.org/10.1084/jem.20021996

Sato, T., N. Onai, H. Yoshihara, F. Arai, T. Suda, and T. Ohteki. 2009. Interferon regulatory factor-2 protects quiescent hematopoietic stem cells from type I interferon-dependent exhaustion. *Nat. Med.* 15:696–700. http://dx.doi.org/10.1038/nm.1973

Shenoi, H., J. Seavitt, A. Zheleznyak, M.L. Thomas, and E.J. Brown. 1999. Regulation of integrin-mediated T cell adhesion by the transmembrane protein tyrosine phosphatase CD45. *J. Immunol.* 162:7120–7127.

Spalinger, M.R., S. Lang, A. Weber, P. Frei, M. Fried, G. Rogler, and M. Scharl. 2013. Loss of protein tyrosine phosphatase nonreceptor type 22 regulates interferon-γ-induced signaling in human monocytes. *Gastroenterology.* 144:978–988: e10. http://dx.doi.org/10.1053/j.gastro.2013.01.048

Stanford, S.M., and N. Bottini. 2014. PTPN22: the archetypal non-HLA autoimmunity gene. *Nat Rev Rheumatol.* 10:602–611. http://dx.doi.org/10.1038/nrrheum.2014.109

Vang, T., M. Congia, M.D. Macis, L. Musumeci, V. Orrú, P. Zavattari, K. Nika, L. Tautz, K. Taskén, F. Cucca, et al. 2005. Autoimmune-associated lymphoid tyrosine phosphatase is a gain-of-function variant. *Nat. Genet.* 37:1317–1319. http://dx.doi.org/10.1038/ng1673

Vang, T., W.H. Liu, L. Delacroix, S. Wu, S. Vasile, R. Dahl, L. Yang, L. Musumeci, D. Francis, J. Landskron, et al. 2012. LYP inhibits T-cell activation when dissociated from CSK. *Nat. Chem. Biol.* 8:437–446. http://dx.doi.org/10.1038/nchembio.916

Velaga, M.R., V. Wilson, C.E. Jennings, C.J. Owen, S. Herington, P.T. Donaldson, S.G. Ball, R.A. James, R. Quinton, P. Perros, and S.H. Pearce. 2004. The codon 620 tryptophan allele of the lymphoid tyrosine phosphatase (LYP) gene is a major determinant of Graves' disease. *J. Clin. Endocrinol. Metab.* 89:5862–5865. http://dx.doi.org/10.1210/jc.2004-1108

Voulgarelis, M., S. Giannouli, A. Tasidou, D. Anagnostou, P.D. Ziakas, and A.G. Tzioufas. 2006. Bone marrow histological findings in systemic lupus erythematosus with hematologic abnormalities: a clinicopathological study. *Am. J. Hematol.* 81:590–597.

Wang, Y., I. Shaked, S.M. Stanford, W. Zhou, J.M. Curtsinger, Z. Mikulski, Z.R. Shaheen, G. Cheng, K. Sawatzke, A.M. Campbell, et al. 2013. The autoimmunity-associated gene PTPN22 potentiates toll-like receptor-driven, type 1 interferon-dependent immunity. *Immunity.* 39:111–122. http://dx.doi.org/10.1016/j.immuni.2013.06.013

Zhang, J., N. Zahir, Q. Jiang, H. Miliotis, S. Heyraud, X. Meng, B. Dong, G. Xie, F. Qiu, Z. Hao, et al. 2011. The autoimmune disease-associated PTPN22 variant promotes calpain-mediated Lyp/Pep degradation associated with lymphocyte and dendritic cell hyperresponsiveness. *Nat. Genet.* 43:902–907.

Zikherman, J., M. Hermiston, D. Steiner, K. Hasegawa, A. Chan, and A. Weiss. 2009. PTPN22 deficiency cooperates with the CD45 E613R allele to break tolerance on a non-autoimmune background. *J. Immunol.* 182:4093–4106. http://dx.doi.org/10.4049/jimmunol.0803317